Energy 360 (2026) 141564

Contents lists available at ScienceDirect

Energy

journal homepage: www.elsevier.com/locate/energy

Assessment of fluid mixtures in transcritical high-temperature heat pumps exploiting waste heat with large temperature glides

Dario Alfani, Ettore Morosini *, Giampaolo Manzolini

Politecnico di Milano, Dipartimento di Energia, Via Lambruschini 4, Milano, 20156, Italy

ARTICLE INFO

Keywords:
High temperature heat pump
Heat pump CO_2 mixtures
Waste heat upgrade
Sensible heat pump
Industrial decarbonization

ABSTRACT

The work investigates innovative compact configurations of high temperature transcritical heat pumps with sensible heat sinks that upgrade sensible waste heat with significant source exploitation. In this context, CO_2 mixtures with heavier dopants are suggested as working fluids to properly match the temperature profile at the evaporator and transcritical cooler. Initially, a methodology is presented to analyze the cycle behavior and optimize its performances by modifying the necessary input parameters: for a representative mixture (CO_2+acetone) and assuming a heat source of 100 °C, performance maps of the different heat pump configurations are reported as a function of the temperatures in the evaporator and cooler. The results obtained highlight that the COP in these conditions largely benefits by using a single-phase expander and by setting the cycle minimum pressure at high values, close to the pressure at the mixture cricondentherm. Then, a case study based on the production of hot pressurized water (140-200 °C) is examined, comparing simulations of the CO_2+acetone mixture with mixtures previously analyzed in literature. It is further underlined that mixtures under these circumstances allow for very limited pressure and volumetric ratios at the compressors, around 2-4, exploiting the heat source for a temperature range much higher than pure fluids. Expanding the analysis to subcritical heat pumps it is demonstrated that these are less favorable than transcritical ones at same boundary conditions, as subcritical solutions present higher mixture maximum temperatures, over the thermal stability limit of the fluid, sub-atmospheric pressures and way higher compressor volume ratios.

1. Introduction

In the industrial sector, excess thermal energy is typically recovered either through direct use, such as for space heating applications, or by means of power cycles like Organic Rankine Cycles (ORC), which convert unexploited thermal power into electricity, which can be either self-consumed or exported to the grid. Nevertheless, for waste heat temperatures below 100-120 °C, the resulting conversion efficiency of these systems generally makes the initial investment cost economically unattractive in most scenarios [1].

Despite this, low-temperature waste heat sources are abundant in a wide range of industrial processes, particularly in the food, chemical, and paper sectors. Estimations of the global industrial waste heat indicate that the majority is released in the form of exhaust gases or by-products effluents from energy-intensive processes, with the largest share occurring at temperatures below 100 °C [2]. Focusing on the European Union, a white paper from KCORC reported that the theoretical potential of waste heat recoverable under 100 °C is 390 TWh_{th}/year, of which the recovery is deemed technically feasible for 32 TWh_{th}/year, representing 21% of all the technically recoverable thermal power [3].

At the same time, it is often required to supply heat in the temperature range above 100 °C, up to 200 °C, for industrial and manufacturing processes, which corresponds to the operating conditions of high temperature heat pumps (HTHP). These systems can upgrade the available waste heat to the required temperature levels, enabling its reuse in the processes, thereby enhancing the energy efficiency and reducing the emissions of these sectors [4]. As a matter of fact, according to a recent white paper, the process heat demand in the European industrial sector in the 100-200 °C range corresponds to 507 TWh_{th}/year, while just 215 TWh_{th}/year are required in the 60-100 °C range [5]. To meet the demand of high-temperature heat, a large number of HTHPs with a duty below 2 MW_{th} are currently installed in the European food sector, as highlighted in a literature review of Marina [6], while those employed in the paper and chemical industry are commonly below 10 MW_{th}.

As HTHPs have been already introduced in the scientific literature as a solution to unlock the potential of low temperature waste heat

* Corresponding author.
E-mail address: ettore.morosini@polimi.it (E. Morosini).

https://doi.org/10.1016/j.energy.2026.141564
Received 8 March 2026; Received in revised form 21 May 2026; Accepted 2 June 2026
Available online 13 June 2026

Nomenclature:

Acronyms

COP	Heat pump Coefficient of Performance
EoS	Equation of State
GWP	Global Warming Potential of a fluid
KPI	Key Performance Indicator
HCFO	Hydro-Chloro-Fluoro-Olefins
HFC	Hydro-Fluoro-Carbons
HFO	Hydro-Fluoro-Olefins
HTHP	High temperature heat pump
HX	Heat Exchanger
ODP	Ozone Depletion Potential of a fluid
sCO_2	Supercritical Carbon Dioxide
SSD	Superheated Steam Dryer
TES	Thermal Energy Storage
VLE	Vapor Liquid Equilibrium of a mixture
VHC	Volumetric Heating Coefficient
VHTHP	Very high temperature heat pump
VR	Volumetric Ratio across the compressor

Symbols

P	Pressure [bar]
ΔP_{HX}	Pressure drop across the heat exchanger [bar]
P_{cricth}	Pressure at the cricondentherm [bar]
P_{sat}	Saturation pressure of the mixture [bar]
T	Temperature [°C]
$T_{mean\ log}$	Logarithmic mean temperature [°C]
T_{max}	Maximum temperature of the cycle [°C]
T_{sat}	Saturation temperature of the mixture [°C]
T_{cricth}	Temperature of the cricondentherm [°C]
ΔT	Temperature difference [°C]
ΔT_{lift}	Temperature lift of the heat pump [°C]
ΔT_{ml}	Logarithmic mean temperature difference [°C]
ΔT_{source}	Temperature difference of the source [°C]
ΔT_{sink}	Temperature difference of the sink [°C]
ΔT_{rec}	Internal pinch point of the recuperator [°C]
h	Specific enthalpy [kJ/kg]
dh	Infinitesimal specific enthalpy difference [kJ/kg]
dP	Infinitesimal pressure difference [Pa]
ρ	Density [kg/m^3]
v	Specific volume [m^3/kg]
η_{iso}^{comp}	Isentropic Efficiency of the compressor
η_{poly}^{comp}	Polytropic Efficiency of the compressor
$\dot{Q}_{HS}$	Thermal power from the heat source [MW]
$\dot{W}_{comp}$	Mechanical power of the compressor [MW]
$\dot{W}_{exp}$	Mechanical power of the expander [MW]
x_{CO2}	Molar CO_2 composition of the mixture [−]

recovery, a literature review of working fluids and HTHP characteristics from literature is shown in Table 1. As the commercial solutions shift away from hydrofluorocarbons (HFC) and olefins (HFO) driven by environmental regulations (e.g., the F-gas and REACH regulations), HTHP can nowadays rely on hydrocarbons (HC), siloxanes and other categories of fluids. Among these, CO_2 is attractive from environmental and safety standpoint but shows thermodynamic limitations with high temperature sources and when large source temperature differences are necessary. CO_2 mixtures can be a solution for compact systems that exploit large temperature glides and lifts, with good matching of the temperature profiles in the evaporator and supercritical cooler with the source and the sink, respectively. Nevertheless, most of the existing studies focus on subcritical layouts and present low temperature glides.

Considering the trends from available literature, it is evident that CO_2 mixtures with organic dopants are of interest for heat recovery processes exploiting sensible heat sources. Zeotropic mixtures with substantial temperature glides allow the working fluid temperature to vary continuously during phase change, better matching the temperature profile of the sensible heat source. This improved temperature matching reduces the average temperature difference in the evaporator, lowering irreversibilities, and increases both the cycle efficiency and heat recovery effectiveness from a given source. This aspect is particularly beneficial if the source can be hypothetically cooled down to ambient temperature.

Extending the interest in industrial applications, specifically of HTHP with sensible heat sinks, examples are already considered in literature. A literature review is proposed and summarized in Table 2, highlighting the technical interest on these systems to clearly justify the objective and motivation of this study. A more detailed overview of the integration between sensible heat sources and sinks for advanced applications with HTHP is also reported by IEA in Annex 58 [21], mentioning additional applications such as thermal separation, thermal treatment and thermal preservation processes in the temperature range above 120 °C. For the applications reported in Table 2, given the high temperature heat to be delivered, HTHPs are adopted specifically to substitute natural gas boilers, drastically reducing the carbon footprint of the process.

According to the literature on HTHP of Table 2, superheated steam drying processes can be coupled with HTHP exploiting latent heat sources, leading to high COP values (typically between 4 and 5, depending from the conditions). Nevertheless, these cycle results are obtained under conditions that don't allow for a large temperature exploitation of the heat source, as they rely on isothermal or near-isothermal evaporation processes at about 100 °C. From this perspective, this study aims at expanding the analysis to include a wider heat source exploitation.

The simulations from literature of spray drying processes aided by HTHP also reports similar behavior: with state-of-the-art components simulations result in COP around 4 with near-isothermal evaporations and heat sources at around 100 °C with organic fluids. Detailed simulations with sCO_2 HTHP are shown in Zühlsdorf's work for spray drying applications: much lower COP (below 2) is found, but the case study is proposed for a condition where the outlet temperature of the heat source around 25 °C, with around 30 °C of source exploitation, being a condition of interest for the simulations proposed in this work.

Due to their favorable thermodynamic properties and phase change behavior, CO_2-dominant binary mixtures can be considered a promising solution for application characterized by both sensible heat sources and sinks, such as the ones discussed in Table 2. These working fluids allow evaporation temperatures compatible with low-temperature waste heat, which is generally available at temperatures up to 100 °C, while featuring high minimum pressures and high average density in the compression process.

Considering the analysis of previous works, two major gaps can be identified with respect to the literature on HTHP with mixtures for advanced applications. First, very large temperature lifts are generally not achieved with conventional vapor compression HTHP in simple cycle configurations, and complex architectures are usually proposed for such applications, independently from the selected working fluid. In contrast, this work investigates working fluids mixtures in a simple HTHP configuration operating at relatively low pressures, close to the cricondenbar. Secondly, highly sensible heat sources are difficult to completely exploit by means of working fluids and mixtures commonly adopted in the literature, where case studies are characterized by temperature glides lower than 20-30 °C. The approach proposed in this work

Table 1
Summary of literature review works on conventional and innovative working fluids for HTHP and respective system characteristics.

Working fluid	Typical temperature level	Cycle configuration	Main advantages	Main limitations	Reference
Water	Up to 100-120 °C	Subcritical	Cheap and easy to handle working fluid; Validated technology	Performances sensible to heat sink temperatures variations above ~100 °C; Extremely low densities and pressures at evaporator; Risks of corrosion	Wu [7]
Pure HFCs (e.g. R245fa, R365mfc)	Up to 120-150 °C	Subcritical	Good thermophysical properties; Mature technology; High efficiency; Non-flammable	Being progressively replaced by low-GWP alternatives and penalized by F-gas regulations	Arpagaus [4]
Pure HFOs/HCFOs (e.g. R1233zd(E))	Up to 150 °C	Mainly subcritical	Low GWP; Not flammable; Suitable replacement for HFCs; Good efficiency in moderate HTHP	Limited adaptability to large temperature glides in sensible heat sources; Low volumetric capacity; Low density at evaporator	Wu [8]
Pure HC (e.g. pentane)	100-150 °C	Subcritical	Natural fluids; Low cost; Good thermodynamic and transport properties	High flammability and safety measurements	Mateu-Royo [9]
Siloxanes and Siloxanes mixtures (e.g. MM, D4)	>150 °C	Subcritical	Thermal stability at high temperatures; high molecular weight	Environmental and safety concerns; Limited glide exploitation; Low density at evaporator; Complex compressor design	Obika [10]
Hydrocarbons (e.g. propane & butane)	110-160 °C	Cascade (Subcritical)	Natural and cheap fluids; Excellent thermodynamic coupling in cascade	Flammabilty in both cycles; Layout Complexity	Bamigbetan [11]
Mixtures HC (butane, pentane, isobutane)	>150 °C	Subcritical	Natural fluids; Low cost; Good heat recovery at medium temperature from heat source; Performance gain with respect to pure fluids	Flammability; High pressures	Hua [12]; Shi [13]
Mixtures HC (butane, pentane, propane)	60-100 °C	Subcritical	Experimental setup: High glides; higher COP than respective pure fluid; Low pressure drop in evaporation	Flammabilty and safety issues	Brendel [14]
Mixtures HC/HFO	Up to 200 °C	Subcritical/ transcritical	Glide adaptation with reduced irreversibility in HX; Consequent higher COP	Potential fractionation of the mixture in two phases	Spale [15]
Mixtures HFO/HFCO	60-100 °C	Subcritical	Experimental setup: High glides; higher COP than pure fluid alternative; more stable COP with variable conditions	Maldistribution of the mixture and composition shift	Brendel [16]
CO_2 + HFO	100-150 °C	Cascade	Very low GWP; Very high temperature lift	Very high pressures; HX complexity e cost	Zhang [17]
CO_2 + Alkanes (butane/pentane)	>115 °C	Cascade	High temperature lifts; Good glide control and optimization; Optimal for hot water production	Flammability; system complexity	Ganesan [18]
CO_2 + Acetone	Up to 220 °C	Subcritical/ cascade	Enables very high delivery temperatures with limited CO_2 fraction	Acetone-dominated mixture with almost latent behavior; Limited sensible source exploitation	Gómez-Hernández [19]
CO_2 + R1234yf	Up to 120-150 °C	Subcritical/ transcritical	Moderate temperature glide	Not suited for very high temperatures; limited source exploitation studied	Zhou [20]

Table 2
Literature review of HTHP used in innovative applications with highly sensible heat sinks.

Application	Description	Sensible Heat Sink		References
		Medium	Temperature	
Superheated steam drying (drying process)	Superheated steam used to dry wet materials (e.g. biomass)	Steam	From 115 °C to 200 °C	Abedini [22], Vieren [23], Bang-Møller [24]
Spray drying (drying process)	Liquid solutions (or slurry) are turned into dried powders of the material fed to the system	Air	From ambient temperature to over 200 °C	Zühlsdorf [25], Wang [26], Vieren [23]
Production of hot pressurized liquid	Process heating utility such as pharmaceutical, food	Pressurized water or thermal oil	Variable range, from a minimum of 100 °C to maximum 200 °C	Vieren [23], Arpagaus [27], Abedini [22]
High temperature district heating networks	Heating of civil sector	Pressurized water	Over 100 °C, depending on location	Barco-Burgos [28], Passamonti [29], Wolscht [30]

addresses this aspect by carrying out a sensitivity analysis on this temperature difference, extending the relevance of the results to a wider range of applications.

To effectively address these literature gaps, this work presents a CO_2-mixture as working fluids by considering a dopant with a lower volatility than carbon dioxide, focusing on a mixture composition that can lead to significantly higher temperature glides and enabling more effective integration with sensible heat sources. The objective of this work is to develop a methodology to analyze the working fluid conditions that can match the temperature levels requirements in a wide range of possible applications, selecting the compressor inlet conditions that can maximize the HTHP performance. In particular, the work focuses on simple recuperative HTHP, with minimum cycle pressures above the atmospheric one, limiting the working fluid inventory and simplifying the inventory management system.

The structure of the analysis proposed in this paper is as follows: Section 2 is dedicated to the methodology adopted to analyze the HTHP systems, with details on the plant layout, working fluid selection and numerical modelling. The results obtained are presented in Section 3 with heatmaps depicting the overall cycle performance over a broad range of boundary conditions, assuming a representative mixture as working fluid. These results demonstrate the wide variety of possible HTHP solutions achievable by fixing the mixture composition. Finally, Section 4 discusses applications related to real case studies, aiming at the maximization of the system performance and heat source utilization, to support progress toward the full decarbonization of the industrial sector.

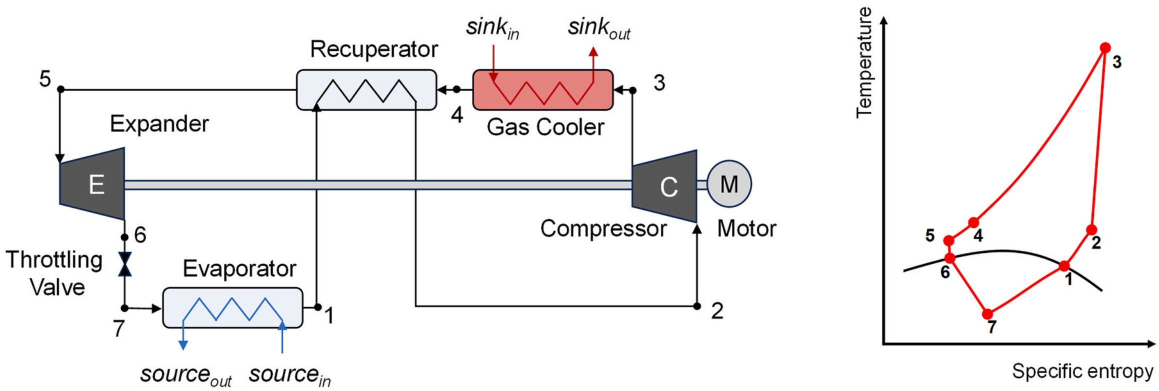

Fig. 1. Schematics of the plant configuration of the simple recuperative transcritical HTHP (left). Corresponding qualitative representation in a Temperature-Specific Entropy diagram (right).

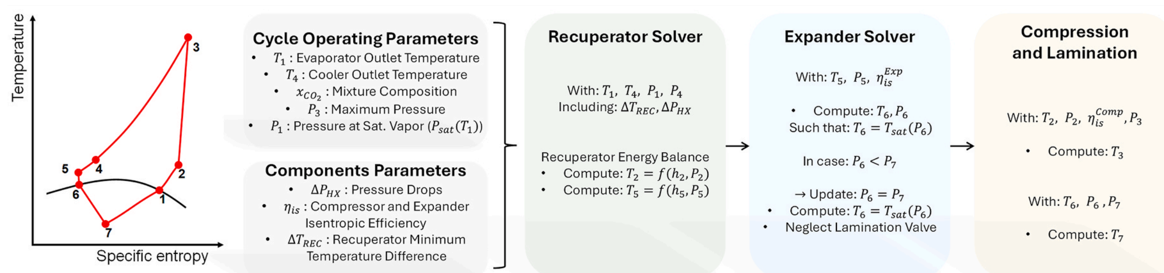

Fig. 2. Workflow adopted for the numerical simulation of the transcritical HTHP.

2. High temperature heat pumps design and optimization

2.1. Investigated cycle layout

This work investigates HTHPs adopting a simple recuperative layout, where an expander is included for the supercritical flow upstream of the throttling valve, as depicted in Fig. 1: a qualitative Temperature-Specific Entropy (T-s) diagram of the HTHP with CO_2-based mixtures is also proposed to approximately describe the fluid behavior in the HTHP. Thanks to the favorable thermodynamic behavior of the selected working fluid mixture, this work demonstrates that achieving high COP and effective heat source utilization does not necessarily require complex system architectures.

As the investigation focuses on applications with heat sources and sinks of large temperature difference, particular attention is given to HTHP configurations characterized by an evaporation process (from point 7 to point 1 in Fig. 1) with a significant temperature variation. In addition, the analysis considers in detail transcritical HTHP configurations with maximum pressures of the cycle set well above the cricondenbar: this technological solution is possible by adopting mixtures with two components of different volatilities. Very high value of high pressures can avoid any issue related to internal pinch point between the working fluid and the heat sink in the supercritical gas cooler (from point 3 to point 4 in the figure), since at these conditions the heat capacity of the mixtures is relatively constant due to the mixing of the two fluid and the high value of the reduced pressures (over 2). As reported in the literature related to CO_2-based HTHP from industrial players [31], [32] and in previous works of the authors on HTHP with CO_2-mixtures [33], [34], high pressures on the hot side of the HTHP are also beneficial from a performance perspective, as they allow for the recovery of mechanical power absorbed by the compressor with an expander (from point 5 to point 6 in the figure). Such component would expand the flow down to the saturation condition, just before entering in the two-phase region and being throttled in a lamination valve, a design choice to preserve the integrity of the expander blades [35], [36], [37].

Finally, a recuperator between the high- and the low-pressure side is considered, which is strongly recommended for applications with a high minimum temperature of the heat sink (proportional to the temperature at point 4 in the figure). This component increases the compressor inlet temperature (from point 1 to point 2), lowering its mechanical consumption at constant compressor outlet temperature, while cooling the flow before the expansion (from point 4 to point 5).

2.2. Methodology for the cycles solution

The HTHP simple recuperative layout is modelled in MATLAB according to the methodology outlined in the flowchart of Fig. 2. The thermodynamic cycle is defined by imposing three main operating parameters: the cycle maximum pressure (P_3), the evaporator outlet condition (T_1), and the cooler outlet temperature (T_4). The first parameter is constrained by the current material technological limitations and components manufacturing. Accordingly, a value of 200 bar is set for all the simulations performed in this study. The second and third parameters are strongly dependent on each specific application and case study: the evaporator outlet temperature is set by the heat source conditions, while the cooler outlet temperature depends on the heat sink inlet temperature. The evaporator outlet condition is always set to saturated vapor, thereby excluding any operative condition in which the low-pressure side of the recuperator operates in the two-phase region or in which the heat source allows for superheating before entering the recuperator.

Compressor and expander isentropic efficiency, pressure drops in the heat exchangers, and the pinch point temperature difference in the recuperator are set as fixed parameters in all the simulations carried out.

In case of heat pump operating with mixtures, an additional degree of freedom is represented by the working fluid composition: the composition is defined starting from the selected CO_2-dopant and the CO_2 mass fraction (identified as x_{CO_2}).

It is also worth mentioning that, as the maximum pressure is fixed at

Table 3
Assumptions for the HTHP components and cycle parameters considered in this work.

Component parameter	Value at design
Compressor Isentropic Efficiency	75%
Expander Isentropic Efficiency	75%
Recuperator Minimum Temperature Difference	5 °C
Gas Cooler Minimum Temperature Difference	5 °C
Evaporator Minimum Temperature Difference	5 °C
Gas Cooler HX Pressure Drop	1 bar
Evaporator Pressure Drop	0.5 bar
Recuperator Pressure Drop (HP/LP)	0.5 bar/1 bar
Cycle Maximum Pressure (P_3)	200 bar
Electro-mechanical Losses	Neglected

the maximum allowable value, the cycle minimum pressure (P_1, defined from T_1 at saturated vapor condition) indirectly determines the compressor pressure ratio, and therefore the compressor outlet temperature (T_3) at a given isentropic efficiency.

Once all the inputs are defined in the HTHP MATLAB model, the code starts by computing all the cycle streams pressures, except for the pressure at the expander outlet, imposing the specified pressure drops in the heat exchangers. Afterwards, the recuperator is solved by imposing the minimum temperature difference between the hot and cold streams (ΔT_{rec}) and solving the component energy balance. In this way, the compressor inlet temperature (T_2) and the expander inlet temperature (T_5) are determined. Afterwards, the expansion of the working fluid is computed by imposing, at given isentropic efficiency, that its outlet is at saturating conditions (P_6, T_6). Finally, the compression and the lamination processes are calculated, finding the two components outlet temperatures (T_3 and T_7).

2.3. Design assumptions and HTHP optimization

The assumptions adopted for the HTHP components, listed in Table 3, are representative of medium-to-large scale systems (MW scale).

The maximum cycle pressure, identified as a key cycle operating parameter and boundary condition (as shown in Fig. 2), is fixed at 200 bar for all simulations. This choice is motivated by the need to limit mechanical stresses on plant components, including piping, and to avoid the adoption of advanced, unconventional and expensive high-strength materials that would be required at higher pressure levels. The value is lower than what considered as upper bound for sCO_2 power cycles in literature, where 250 bar are normally assumed in the literature of concentrated solar or nuclear plants [38] and also adopted as maximum pressure in demonstrator plants under operation [39]. Moreover, these high pressure values are also adopted for pure CO_2 HTHP operating in temperature ranges similar to the ones of this work [40]. The pressure drops are representative of well-designed heat exchangers, characterized by large heat transfer surfaces and limited working fluid velocities. As explained in Section 2.2, the maximum temperature of the working fluid (i.e., the compressor outlet temperature) is not specified as an input, but rather results from the simulations and is monitored during post-processing. The internal temperature difference across the recuperator is set at 5 °C, a reasonable value considering printed circuit heat exchanger as suitable technological solution for applications with high-density fluids.

Due to the moderate volumetric and pressure ratio of both turbomachinery, an isentropic efficiency equal to 75% is assumed for both the expander and the compressor [22]. Preliminary simulations performed by Echogen Power Systems on CO_2 compressors operating with subcritical intake conditions indicate that isentropic efficiencies of up to 80% can be achieved. Since these simulations refer to pressure and volume ratios higher than those considered in this work, the efficiency values adopted in this analysis can be regarded as technically feasible [41]. As common in system-level analyses, both the HXs and the turbomachinery are considered adiabatic, neglecting thermal losses to the environment. Furthermore, off-design performance and transient operation of the cycle are not considered in the present work.

This work proposes two distinct sets of simulations of HTHPs operating with CO_2-based working fluid mixtures. In the first set, the coupling with the heat sink and heat source is not explicitly considered nor modelled, and the analysis focuses exclusively on the cycle performance and the working fluid operating conditions. In the second set, the focus is shifted towards realistic industrial case studies, investigating the optimal integration of the HTHP with available waste heat source and fixed heat sink. In this second part of the work, a 5 °C internal temperature difference is assumed between the working fluid and the cold source and heat sink streams, at the evaporator and at the supercritical cooler, respectively.

2.4. Investigated working fluid and thermodynamic modelling with EOS

Among the possible dopants for CO_2, the adoption of additives with higher molecular mass and normal boiling point at much higher temperature than CO_2 can favor HTHP configurations for applications characterized by large temperature glides, since even a small quantity of dopants in the mixtures is normally sufficient to achieve the desired target in temperature glides of the working fluid. It must be stressed that a key advantage of working fluid mixtures is related to the possibility of fine-tuning their composition to achieve specific thermophysical characteristics tailored to the target application. By carefully selecting the type and concentration of dopant, it is possible to adjust crucial thermodynamic properties such as critical temperature, specific heat capacity, density, and phase-change behavior. This flexibility allows for the optimization of HTHP performance, as the right mixture composition can ensure an optimal matching between the working fluid temperature profile and that of the heat source or sink, thereby enhancing heat exchanger effectiveness and reducing heat transfer exergy losses.

Beyond thermodynamic optimization, the mixture composition can also be adjusted to align with environmental and safety considerations. By selecting low-GWP and zero-ODP dopants, it is possible to develop working fluids that comply with stringent environmental regulations while maintaining high performance. This is particularly relevant in the context of phase-down measures on HFCs and other synthetic refrigerants with high environmental impact. This expected improvement in performance, environmental sustainability, and plant safety highlights the potential of CO_2-based mixtures as a viable alternative to conventional working fluids in the field of HTHP applications. While focusing on non-toxic, non-reactive working fluids and CO_2-dopants, also the risks associated to flammability are inherently mitigated by the dominance of CO_2 in the mixture, a natural fire suppression agent.

The working fluid investigated in this work is the CO_2+acetone mixture (CAS number of acetone: 67-64-1), already proposed in literature as discussed in the introduction. Acetone critical conditions are at 235 °C and 47 bar. As the critical temperature is noticeably higher than that of CO_2 (31 °C), a little fraction of acetone in the mixture is sufficient to bring the cricondentherm above 100 °C, leading to high compressor inlet densities and pressures. With a strong molecular interaction between the two fluids and the important temperature glide, the evaporation trend in a T-Q diagram is more linear with respect to other CO_2+HC mixtures at high pressure conditions, near the critical one. Thermodynamic calculations highlight also a particular feature in T-Q diagrams of the evaporator, showing that by imposing a pinch point in the HX it is found that the temperature difference across the whole profile is always maintaining very low, close to the minimum pinch point value and minimizing irreversibilities related to heat transfer. As reported in the introduction, the mixture is firstly proposed by Gómez-Hernández [19] for a similar temperature range of the sink. Nevertheless, Gómez-Hernández calculations focus on mixture compositions dominant in acetone with subcritical layouts, reaching very high

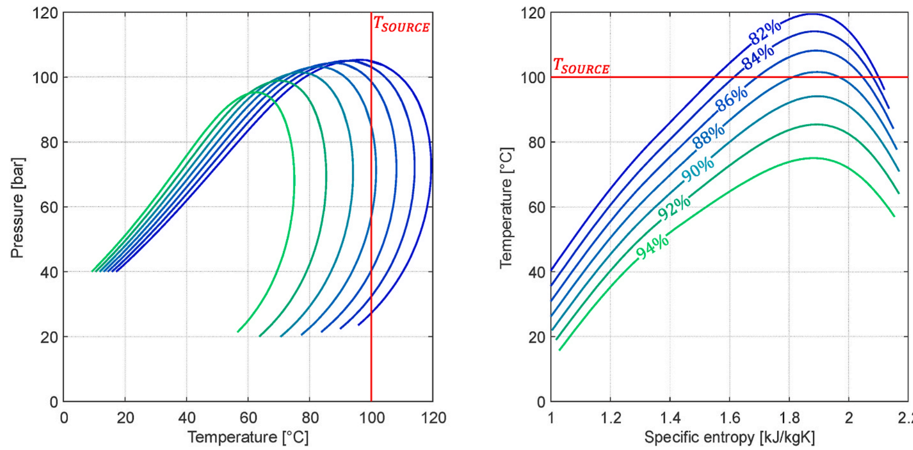

Fig. 3. Extension of the two-phase region of the CO_2+acetone mixture in a composition range close to the design value of $90\%_{mol}$. Heat source temperature of 100 °C (red line). P-T diagram (left), T-s diagram (right). Percentage values refer to molar composition of CO_2 in the mixture CO_2+acetone.

compressor outlet temperatures with pressures below 50 bar: for this reason, a comparison between subcritical layouts with acetone-dominant compositions and transcritical layouts with CO_2-dominant compositions is also shown in this work to assess their differences.

Regarding thermal stability of the dopant, pure acetone exhibits thermal cracking above 400-450 °C and polymerization effects typically above 250 °C. However, in a CO_2-dominant mixture, the high concentration of CO_2 dilutes the dopant, reducing the frequency of acetone molecules collisions required for polymerization reactions. It must be also noted that thermal stability is heavily dependent on material compatibility. For this reason, carbon steel should be avoided at the compressor outlet and materials such as stainless steel (or more expensive Inconel) with passive chromium-oxide layers could be employed to ensure chemical compatibility with acetone. Furthermore, the residence time of the mixture in the high-temperature zone (200-250 °C) is limited due to the heat sink configuration (pressurized liquid HX), which limits the kinetics of potential degradation reactions. It must also be noted that large-scale plants typically employ fluid filters and purging systems to manage any potential fluid residues during cyclic operations.

Regarding oxidation and corrosion risks are in principle not a threat if oxygen and humidity, respectively, are not introduced in the fluid loop: we believe this assumption is reasonable for the system considered.

On the other hand, phase separation is primarily a risk during evaporation, so with a specific evaporator design (in-tube flow) with turbulent flow the fractionation risk is mitigated.

The thermodynamic and transport properties of the working fluid are estimated by means of MATLAB calls of REFPROP v.10, adopting the GERG-2008 equation of state (EoS) by Kunz and Wagner [42] with the binary interaction parameters proposed by Cullimore [43], as the default modelling method of REFPROP v.10. Acetone presents a GWP of 0.5 (lower than CO_2), and no ODP. Other working fluids are also considered in the second set of this work results, based on HTHP case studies available in the literature, and their performance will be compared with that of the CO_2+acetone HTHP. Also in these conditions, REFPROP v.10 is adopted and the default EoS in the tool is used.

2.5. Key performance parameters of the HTHP

The performances of the HTHP are defined with the set of key performance indicators (KPI) listed from Eq. (1) to Eq. (5). The COP, evaluated according to Eq. (1), is computed accounting for the positive contribution of the expander to the reduction of the compression work, a key feature that can significantly improve the overall system performance.

In the first analysis proposed in Section 3.1, the exploitable temperature difference of the sensible heat source (ΔT_{source}) is defined from the temperature difference of the working fluid during the evaporation process, as no internal pinch point constraints are considered. This assumption generally holds true if CO_2-based mixtures with a heavy dopant are employed, since their low volatility relative to CO_2 leads to large temperature glides and nearly monotonic temperature profiles during evaporation, thereby limiting the occurrence of internal pinch points [33]. The compressor volumetric ratio (VR_{comp}) and the HTHP volumetric heating capacity (VHC), are key parameters for assessing the advantages of the innovative CO_2-mixtures in the turbomachinery design, particularly when compared to conventional pure working fluids, such as natural refrigerants. Finally, the temperature lift of the HTHP (ΔT_{lift}) is directly related to the system capability to deliver heat at high temperature, a crucial requirement for applications where decarbonization targets cannot be currently met by conventional heat pumps adopting subcritical layouts with pure fluids or mixtures characterized by limited temperature glides. Considering the first set of results in Section 3.1, where no heat sink and source is defined, the ΔT_{lift} is computed by considering the difference in mean logarithmic average of the temperature of the working fluid in the evaporator and gas cooler.

$$COP = \frac{\dot{Q}_{sink}}{\dot{W}_{comp} - \dot{W}_{exp}} = \frac{h_3 - h_4}{(h_3 - h_2) - (h_5 - h_6)} \tag{1}$$

$$\Delta T_{source} = T_1 - T_7 \tag{2}$$

$$VR_{comp} = \rho_3 / \rho_2 \tag{3}$$

$$VHC = \frac{\dot{Q}_{sink}}{\dot{V}_{in,comp}} = \rho_2 \cdot (h_3 - h_4) \tag{4}$$

$$\Delta T_{lift} = \frac{T_3 - T_4}{\ln\left(\frac{T_3}{T_4}\right)} - \frac{T_1 - T_7}{\ln\left(\frac{T_1}{T_7}\right)} \tag{5}$$

3. Sensitivity analysis of transcritical HTHPs at constant mixture composition

The first set of results of this work in Section 3.1 are computed applying the methodology shown in Fig. 2 to compute the performance of a reference CO_2+acetone mixture suitable for HTHP, covering a wide range of operating conditions. Particular relevance is placed on the sensitivity of the cycle behavior to the evaporator outlet pressure (P_1), and the HTHP performance is presented through contour maps at constant working fluid composition, varying the cooler outlet temperature T_4 and the evaporator outlet pressure P_1. As the evaporator outlet

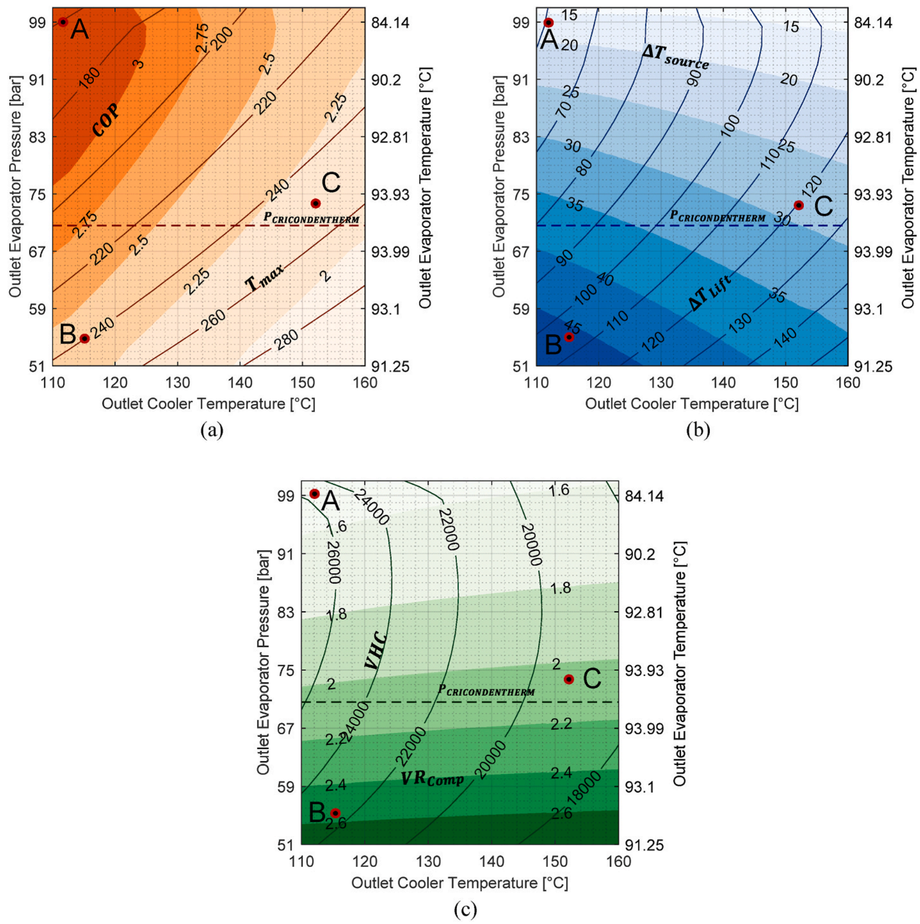

Fig. 4. Heatmaps of the HTHP characteristics with the $90\%_{mol}$ CO_2 + $10\%_{mol}$ acetone mixture (methodology of Fig. 2). COP and Compressor outlet temperature T_{max} [°C] (a), ΔT_{source} [°C] and ΔT_{lift} [°C] (b), VHC [kJ/m^3] and VR (c) for different values of cycle minimum pressure (P_1) and cooler outlet temperature (T_4).

conditions are set to saturated vapor, the corresponding temperature is also defined. However, when operating on the low-pressure side close to the pressure of the mixture at the cricondentherm, the pressure-temperature (P-T) relationship becomes non-monotonic at saturated vapor, and large variations in pressure correspond to very limited differences in saturated vapor temperature.

3.1. Results: CO_2 + acetone mixture in HTHP with 100 °C sensible heat source

This section proposes simulations of HTHP with a mixture composition of $90\%_{molar}$ CO_2 + $10\%_{molar}$ acetone (close to $87\%_{mass}$ CO_2). The heat-source temperature of 100 °C is selected, being representative of low-grade industrial waste heat streams that can be available in the industrial sector. The mixture composition is chosen according to the conditions of the cricondentherm (around 70 bar and 94 °C): this feature makes the working fluid suitable to be exploited in a HTHP with a heat source at 100 °C, bringing a reasonable temperature difference at the evaporator, higher than 6 °C in any conditions and never above 16 °C.

For representation purposes, the T-s and P-T diagrams of the saturation dome of the mixture for CO_2 molar compositions from 82% to 94% are shown in Fig. 3: compositions richer in CO_2 (i.e 94%) are possible for HTHP with heat sources of 100 °C, but under these conditions the cold-end temperature differences at the evaporator would result 25-30 °C, introducing relevant irreversibilities in the heat exchange process at the evaporator. On the other hand, by setting the evaporator outlet (thus the recuperator inlet) at dew point conditions, compositions richer in acetone (i.e 82% CO_2 molar fraction) would not be possible with heat sources at 100 °C due to the large extension of the two-phase region that would reduce the cycle minimum pressure significantly, turning the transcritical cycle into a subcritical one.

Following the methodology of Fig. 2, results of HTHP simulations with a sensible heat source at 100 °C are presented in Fig. 4 in the form of heatmaps: the results show the range of achievable operating conditions of the HTHP operating with a mixture at constant composition and fixed maximum pressure (200 bar). An horizontal dotted line is shown in all the heatmaps of Fig. 4 to define the pressure (left y axis) and temperature (right y axis) of the cricondentherm: all the transcritical HTHP of the heat maps below the dotted line will have a minimum pressure above the pressure of the cricondentherm, while all the HTHP from conditions above the dotted line represents simulations with the cycle minimum pressure higher than the pressure of the cricondentherm.

Considering the results of Fig. 4.a at constant maximum pressure (200 bar) it is evident that increasing the evaporator outlet pressure (left y-axis) leads to higher average temperatures of heat introduction, lower temperature lifts, and thus higher COPs. This behavior is mainly related to the reduction of the compressor pressure ratio, lowering the specific compression work and hence the compressor outlet temperature.

However, this improvement in first law efficiency comes at the expense of reduced heat source exploitation, as shown in Fig. 4.b, mainly due to the smaller evaporation temperature glide ΔT_{source}. This makes high evaporation pressure operating conditions less suitable for applications where effective cooling and exploitation of the available waste heat streams are required.

From a turbomachinery point of view, the reduction in pressure ratio also leads to a marked decrease in the compressor volumetric ratio VR_{comp}, as illustrated in Fig. 4.c. However, across the entire operating range investigated, the compressor volumetric ratio values remain

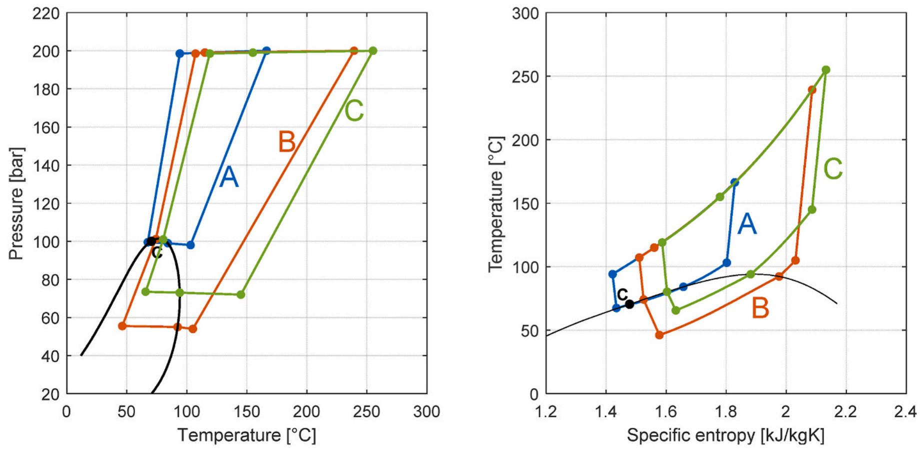

Fig. 5. Pressure-Temperature and Temperature-Specific Entropy diagrams of the representative working fluid (90%$_{mol}$ CO_2 + 10%$_{mol}$ acetone) and the three HTHPs underlined as example in Fig. 3. The effect of a variation in cycle minimum pressure is clearly visible.

limited, always between about 1.5 and 2.7. This is particularly advantageous for compressor design, as lower VR_{comp} values lead to reduced stage loading, improved mechanical reliability, and simpler machine design and layouts. At the same time, the volumetric heating capacity *VHC* is not really affected by variations of the evaporator outlet pressure. This occurs because the increase in compressor inlet density associated with higher pressures is counterbalanced by the reduction in the thermal power delivered to the sink. Overall, these trends highlight a fundamental trade-off enabled by the thermodynamic of the working fluid: increasing evaporator pressure favors efficiency and compact turbomachinery, while lower evaporator pressures enhance waste heat exploitation and delivered thermal power, allowing the CO_2+acetone mixture at constant composition to be adapted to different industrial contexts simply by varying the HTHP operating conditions.

On the other hand, increasing the cooler outlet temperature T_4 (x-axis) shifts the heat rejection process towards higher temperature levels, thereby increasing the average temperature at which heat is delivered to the heat sink. For the recuperative layout with fixed recuperator pinch point temperature difference, this effect is even more pronounced as an increase in the cooler outlet temperature T_4 indirectly raises the compressor inlet temperature T_2. As a consequence, the compressor outlet temperature T_{max} also increases, boosting the average heat rejection temperature and the overall temperature lift of the HTHP, leading to an unavoidable penalization of the COP.

From a turbomachinery perspective, the compressor volumetric ratio remains nearly constant since both the compressor inlet and outlet density slightly decrease, as pressures of the cycle are fixed but the compression process takes place at higher temperatures. Differently, the volumetric heating capacity (VHC) decreases markedly with increasing cooler outlet temperatures (x-axis). The rise in compressor inlet temperature reduces the working fluid density at suction, leading to lower thermal power per unit volumetric flow rate.

Focusing on the performance of the HTHP with the CO_2+acetone mixture (90 % mol CO_2), three representative cycles are selected to illustrate how variations in minimum pressure and cooler outlet temperature affect system behavior. Cycles operating with a minimum pressure below the pressure of the cricondentherm (dotted line in Fig. 4), such as cycle “B”, fall below this line, whereas cycles “A” and “C” have minimum pressures above it.

Pressure-temperature plots for these three representative HTHPs are shown in Fig. 5, providing a clearer visualization of how variations in minimum pressure and maximum cycle temperature affect the overall cycle behavior. Corresponding temperature-entropy diagrams are also included to further highlight the differences between the cycles while keeping the working fluid composition constant.

Focusing on the three HTHP configurations visualized in Fig. 5, their characteristics and possible applications are discussed in the following:

- Cycle “A” represents a configuration with the minimum cycle pressure above P_{cricth} and a relatively small pressure ratio (around 2). The throttling valve is absent because the expansion, when considered down to the cycle minimum pressure, allows the expander outlet conditions to remain in single-phase region: in this condition the valve is not required since the flow is already at the minimum pressure (referring to the blue cycle in the P-T diagram of Fig. 5), easing the flow distribution in the manifold of the evaporator. Cycle “A” is also characterized by a relatively small temperature lift (60 °C), leading to a high COP (about 3.2) but also a low compressor outlet temperature (165 °C). Evaporation occurs close to the mixture critical point, resulting in a smaller temperature glide along the process (18 °C) and limiting the effective exploitation of sensible heat sources. At the same time, the compressor volumetric ratio is below 1.5 due to the high minimum cycle pressure, and the VHC is above 25 MJ/m^3 thanks to the low cooler outlet temperature. In summary, cycle “A” is optimized for maximum COP and eased turbomachinery design, suitable for applications where efficiency is prioritized over maximizing heat source utilization.
- Cycle “B” is selected with a cooler outlet temperature similar to cycle “A”, but with the cycle minimum pressure set below the cricondentherm pressure P_{cricth}, to properly highlight the sensitivity of the cycle performance to this parameter. Compared to cycle “A”, the pressure ratio increases, as well as the cycle maximum temperature (240 °C). The higher temperature lift, above 100 °C, results in a lower COP (about 2.4) but also a better exploitation of the heat source, with an evaporation temperature glide of 45 °C. The compressor volumetric ratio rises to 2.6, while VHC remains relatively high at 23 MJ/m^3. The throttling valve is present, and the evaporator inlet operates fully in the two-phase region, with a very small heat duty required by the recuperator. From an application perspective, cycle “B” is particularly suitable for processes requiring substantial heat upgrade from moderate-to low-temperature waste streams, such as advanced drying operations. Here, byproducts or intermediate streams from the drying plant can serve as the heat source, allowing the HTHP to maximize heat recovery and temperature lift, at the expense of a COP penalty compared to Cycle “A”. This illustrates a key trade-off in CO_2-mixture HTHPs: maximizing source exploitation and temperature lift often requires higher pressure ratios and lower COPs, which can be mitigated by careful mixture design and selection of the cycle operating conditions.
- Cycle “C” is selected with a very high cooler outlet temperature (T_4, over 150 °C) resulting in a maximum working fluid temperature of 250 °C, close to the thermal stability limit of the working fluid.

Table 4
Characteristics of the heat source and heat sinks for the application of HTHP considered in literature by Abedini [22] and Vieren [23].

Parameter	Heat source	Heat sink
Fluid/Heat Carrier	Water	
Mass Flow Rate	30 kg/s	Maximized
Inlet Temperature	110 °C	140 °C
Outlet Temperature	Minimized/Optimized	200 °C
Pressure	3 bar	55 bar

Increasing T_4 raises the average temperature of heat rejection, which consequently increases the temperature lift (ΔT_{lift} around 120 °C). A larger ΔT_{lift} allows the HTHP to deliver heat at higher temperatures but simultaneously increases the compression work, thus penalizing the COP when compared to cycles "A" and "B". The evaporation process is set close the cricondentherm pressure of the mixture, leading to a relatively limited temperature glide (30 °C), and thus penalizing heat source utilization. This makes the configuration suitable for applications where delivering high-temperature heat is more important than maximizing the cooling of the source. Due to the high cooler outlet temperature, the compressor inlet temperature increases with respect to cases "A" and "B" due to the fixed pinch in the recuperator. As a result, the density of the working fluid at the compressor inlet slightly reduces, and the VHC is slightly penalized. On the other hand, VR_{comp} remains limited as the minimum cycle pressure is above P_{cricth}, and the maximum cycle pressure is fixed at 200 bar. This makes the compressor design manageable and avoids excessive pressure ratios that could compromise mechanical reliability. Cycle "C" represents a high-temperature, high-lift operation that is ideal for industrial processes that are currently difficult to decarbonize (e.g., chemical synthesis, high-temperature drying). It must be noted that operating near 250 °C requires careful attention to long-term thermal stability of the CO_2 + acetone mixture. At such conditions, the organic dopant may undergo thermal degradation, potentially altering thermophysical properties and affecting the reliable operation of HTHP components. Therefore, appropriate operational limits must be defined to ensure safe and stable system performance over extended operating periods.

The analysis carried out demonstrates that the given working fluid can be effectively adapted to different HTHP applications and boundary conditions just by adjusting the compressor inlet operating conditions.

As a consequence, it becomes relevant to carry out an additional analysis in which the application is specified, whereas the mixture composition is varied as an optimization parameter.

To do so the next section introduces a case study in which the heat source and heat sink characteristics are defined and fixed, reflecting a realistic industrial case-study, while the working fluid composition is systematically tuned to the specific application requirements. This approach highlights the flexibility of the proposed methodology in adapting CO_2-based mixtures to practical operating conditions of interest for the industrial sector.

4. HTHP for production of pressurized hot water at variable mixture composition

Following the sensitivity analysis discussed in the previous section, which highlighted the strong dependence of HTHP performance on operating parameters, the second set of results in this section applies the proposed methodology to a real industrial case study with predefined heat source and sink conditions.

The case study selected, already discussed in the literature review of this work, is reported by Abedini [22] and Vieren [23] based on surveys conducted with industrial stakeholders in Belgium. For this case study, high temperature sensible heat is required up to 200 °C. Many industrial sectors, including pharmaceuticals and food processing, currently meet this demand using conventional natural gas boilers, which continuously reheat water as it circulates through the process. By replacing the boiler with an HTHP, an available waste heat source can be recovered and upgraded, significantly cutting fuel consumption, increasing the industrial site overall energy efficiency and reducing its CO_2 emissions.

According to literature, in this case study a stream of pressurized water at 55 bar represents the heat sink, which must be heated from 140 °C to 200 °C, while the available heat source is an unexploited hot water stream at 110 °C and 3 bar, as summarized in Table 4. As mentioned in Section 2.3, these HTHP simulations include an additional constraint on the pinch point temperature difference at the evaporator and the supercritical cooler, assumed fixed at 5 °C, to explicitly account for realistic heat exchanger temperature profiles.

Results of HTHP with mixtures for this case study were already reported in Abedini's work [22]. As such, a validation of the developed numerical model with the results of working fluid mixtures by Abedini is shown in Appendix, highlighting a good agreement.

Nevertheless, the authors considered only the COP as KPI of the system, without including the effect of the exploitation of the heat source. Differently, this work highlights conditions where the outlet temperature of the heat source is minimized, maximizing the thermal power recovered from the waste heat stream. Thus, the mass flow rate of the heat sink (heated from 140 °C to 200 °C) is not a boundary condition of the optimization problem, but it is maximized by optimizing the HTHP working fluid mass flow rate. This approach prioritizes the useful effect of the heat pump (i.e. the thermal power delivered to the cold sink), at the expense of a moderate increase in compressor electrical consumption, thus explicitly addressing the trade-off between efficiency and useful heat recovery.

A second important difference between Abedini's results and this work is related to the working fluid selection, as this work focuses on a CO_2-mixture with a less volatile dopant, leading to a transcritical HTHP configuration. In contrast, Abedini's work [22] proposes mainly subcritical HTHPs, using mixtures whose components exhibit similar volatility. This distinction is particularly relevant for applications involving highly sensible waste heat sources, where large temperature glides during evaporation can significantly enhance the heat source exploitation. Finally, although Abedini's work also reports two additional case studies, these involve latent heat sources. Such sources are generally more suited to HTHP working with pure fluids, due to the favorable coupling between isothermal phase change and the heat source temperature profile, and are therefore not considered in the present analysis.

According to Abedini's results on HTHP with mixtures for the application shown in Table 4, temperature glides during evaporation generally do not exceed 20 °C (with a single exception, being the ethanol/m-xylene mixture), corresponding to a similar heat source exploitation between various mixtures. Thus, for a waste heat source entering at 110 °C, the outlet temperature remains close to 90 °C, limiting the exploitation of sensible heat and intrinsically constraining the thermal power delivered to the heat sink. For this reason, consistently with the results of Section 3.1, the CO_2-based mixture investigated in this work is proposed to achieve much larger temperature glides during evaporation, enabling improved cooling of the heat source and higher useful thermal power delivered to the sink.

In particular, the calculations for this case study are carried out according to the following methodology:

- As a CO_2-dopant is identified, the modelling of the mixture behavior with EoS can point to a reasonable composition range: this is possible by considering the heat source inlet temperature and the minimum pinch point temperature difference at the evaporator (5 °C).

  In particular, the evaporator outlet temperature (T_1, referring to Fig. 1) can be defined across the composition range such that it is lower than the temperature of the cricondentherm (T_{cricth}) and higher

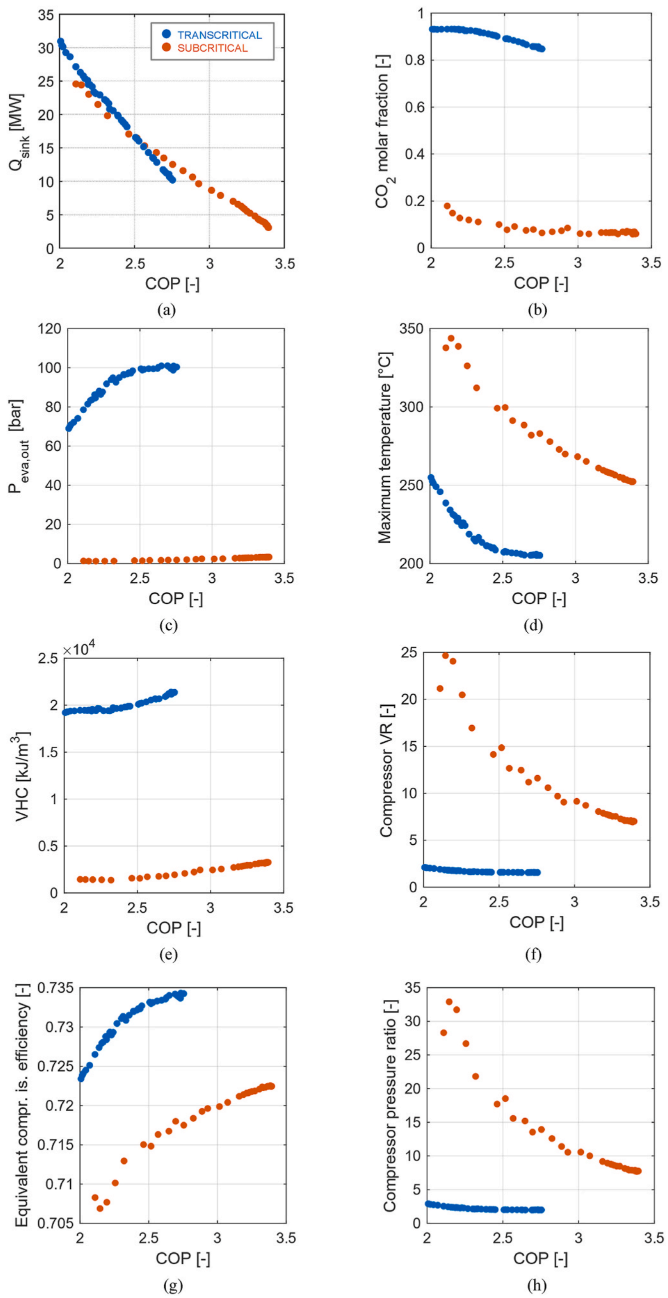

Fig. 6. Trend of the COP and other HTHP characteristics and KPI with the CO_2+acetone mixture as working fluid for the application defined in Table 4. Blue points refer to transcritical HTHP, orange points to subcritical HTHP.

than the critical temperature of the mixture. As such, referring to the results of Fig. 4 of the previous analysis, conditions of transcritical HTHP where the minimum pressure is lower than the pressure at cricondentherm can be considered of minor interest, as they lead to unfavorable COP ranges.

- Across this admissible composition range, HTHP simulations are carried out, matching the required temperature range at the heat sink and accounting for the pinch point constraint also in the supercritical cooler.
- The resulting solutions are organized based on COP and recovered thermal power from the heat source, the latter being directly related to the waste heat stream temperature difference across the evaporator.

This approach clearly highlights the trade-off between COP (i.e. electric consumption) and useful thermal power delivered to the sink, which is discussed through Pareto fronts in the following section. Both transcritical and subcritical HTHP solutions are compared, emphasizing the differences between the two different configurations in terms of performance, operating conditions, and key design parameters.

4.1. Results: case study for pressurized hot water production from 140 °C to 200 °C

The results of the case study producing hot water from 140 to 200 °C with HTHP adopting the CO_2+acetone mixture are shown in Fig. 6, highlight the trade-off between the COP of the system and the useful thermal power delivered to the sink, $\dot{Q}_{sink}$. Simulations both under transcritical configuration (shown in blue in Fig. 6) and subcritical configuration (shown in orange) are carried out, with the aim of highlighting the impact of mixture composition and cycle layout on both performance and operating characteristics. With the mixture adopted and the specified boundary conditions of the heat source, the transcritical configurations operate with a CO_2-dominant working fluid mixture, similar to those presented in Section 3.1, while the subcritical configurations result to be acetone-dominant.

The assumptions on cycle characteristics necessary for the simulations, such as heat exchangers pressure drops and pinch point temperature differences, are analogous to the ones reported in Table 3, with the sole exception of the compressor efficiency. In this section, a polytropic compressor efficiency of 75% is considered for all the simulations, rather than a fixed isentropic efficiency as proposed in Section 3.

A constant polytropic efficiency describes the local quality of the compression process on an infinitesimal basis and is therefore independent of the overall pressure ratio. This property makes it a more physically consistent assumption across the wide range of pressure ratios investigated in this work, from about 2 in the transcritical configurations up to over 30 in the subcritical ones. The polytropic efficiency η_{poly}^{comp} is formally defined as reported in Eq. (6).

$$\eta_{poly}^{comp} = \left(\frac{dh_{is}}{dh}\right)_{path} = \frac{vdP}{dh} \tag{6}$$

in this equation dh_{is} and dh are the isentropic and actual enthalpy increments associated with the infinitesimal pressure increase dP along the compression path, while v is the specific volume of the compressed fluid.

In the simulations, the polytropic efficiency modeling is implemented numerically by discretizing the overall pressure ratio into 100 equal steps and updating the thermodynamic state at the outlet of each step computing the compression with an isentropic efficiency value equal to the polytropic one. The corresponding overall isentropic effi-

Table 5
Range of operating conditions used in the Pareto analysis of Fig. 5.

Parameter of the Optimization	Transcritical Cycles Range	Subcritical Cycles Range
CO_2 molar fraction	80% – 98%	5% - 40%
Cricondentherm Temperature [°C]	94 - 124	186 - 223
Evaporator hot end ΔT ($T_{in,source} - T_1$) [°C]	5 – 40	5 - 40

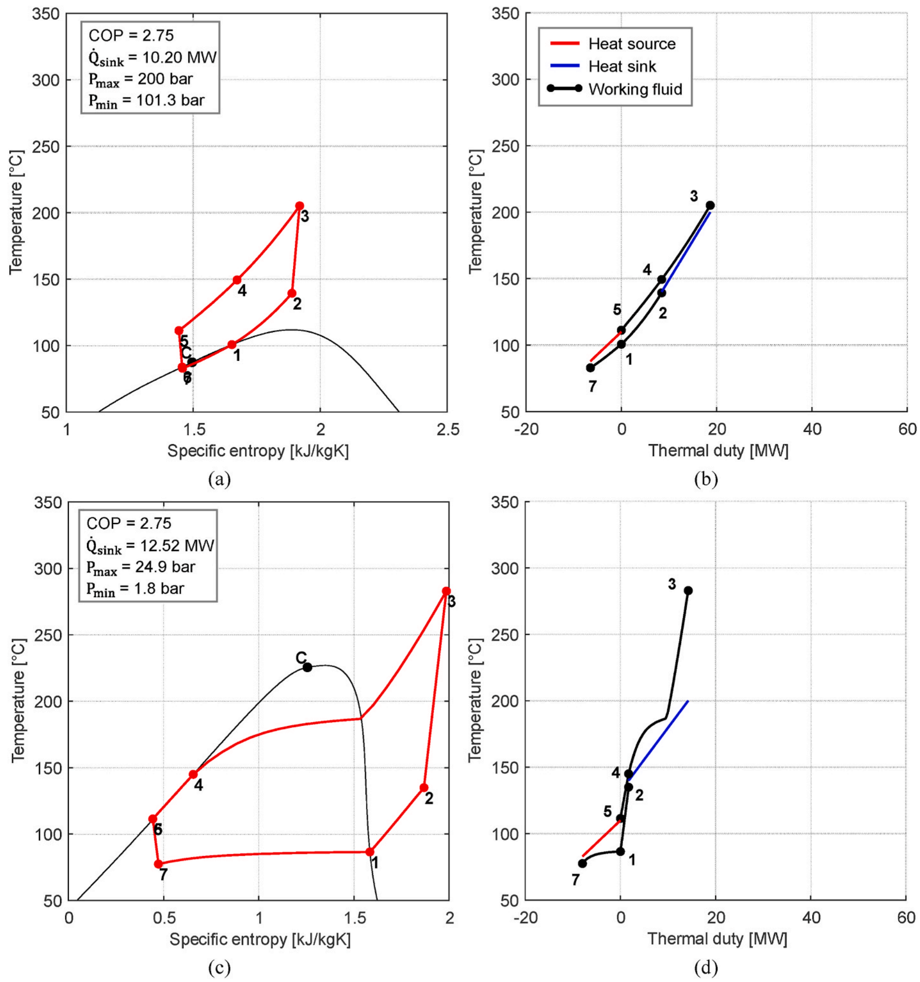

Fig. 7. HTHP from the Pareto front analysis of Fig. 6 with COP values around 2.75. Fig a, c) T-s diagrams of the cycles, b, d) T-Q diagrams of the HXs (evaporator, recuperator and cooler). CO_2-dominant mixtures in Fig a, b) with transcritical conditions, acetone-dominant mixtures in c, d) with subcritical ones.

ciency is computed using Eq. (7) a posteriori and reported among the results to allow a direct evaluation of the assumed compression quality. In the equation $h_{out,is}$ is the outlet isentropic enthalpy, computed from P_{out} and s_{in}.

$$\eta_{iso}^{comp} = \frac{h_{out,is} - h_{in}}{h_{out} - h_{in}} \tag{7}$$

The choice of a fixed value for the compressor polytropic efficiency helps in comparing HTHP conditions at variable isentropic efficiency but at same aerodynamic quality of the compressor stages. This assumption is necessary since the study doesn't address quantitative characterizations on the number of stages necessary to efficiency achieve the compression, nor on the rotational speed of each stage.

Focusing on the results in Fig. 6, they are the outcome of a multi-objective optimization, whose boundary conditions are reported in Table 5. The results are presented in the form of Pareto fronts, and among all the simulated solutions, for each value of COP only the configuration delivering the maximum thermal power to the sink is presented. With respect to the case study of Abedini (also characterized in Table 4), in the present work the pinch point temperature difference at the HTHP evaporator is fixed at the minimum value of 5 °C, whereas the temperature difference at hot end is varied in a range from 5 °C up to 40 °C in the optimization, analyzing a broader range of possible solutions.

As visible from the results the values of COP and $\dot{Q}_{sink}$ are inversely proportional, since a higher useful power can only be obtained at the expense of a lower COP and higher electric consumption. This behavior is mostly due to the larger heat source exploitation ΔT_{source} which, at constant heat source mass flow and inlet temperature, lead to an increase of the HTHP temperature lift and penalize the second law efficiency. At the same time, a larger ΔT_{source} implies a larger HTHP thermal input $\dot{Q}_{source}$, which directly translates into a higher thermal power delivered to the sink $\dot{Q}_{sink}$.

For the given heat source inlet temperature of 110 °C, the Pareto analysis identifies optimal CO_2 molar fractions in the range 87-92 % for the transcritical configurations achieving moderate COP values (between 2 and 2.5), but with thermal powers delivered to the sink exceeding 18 MW_{th}, and as high as 31 MW_{th}. It is thus evident that transcritical CO_2-rich mixtures are the preferable solution when maximizing waste heat recovery is the primary objective. On the contrary, operating points with COP values above 2.5 but a lower delivered thermal power ($\dot{Q}_{sink}$ <18 MW_{th}) are predominantly associated with subcritical configurations (with resulting CO_2 molar fractions in the range 6-18 %), indicating that these solutions are theoretically preferrable when electrical efficiency is considered the only KPI, regardless the technical feasibility of the solution.

The figures also depict the working fluid pressure at the evaporator outlet (i.e. the cycle minimum pressure, Fig. 6.c), the maximum temperature (at compressor outlet, Fig. 6.d), the VHC of the HTHP (Fig. 6.e), the compressor VR (Fig. 6.f) and pressure ratio (Fig. 6.h). Subcritical configurations have much lower values of compressor inlet pressures and must elaborate a substantial compressor pressure ratio to satisfy the heating needs reported in Table 4: given also a very different working

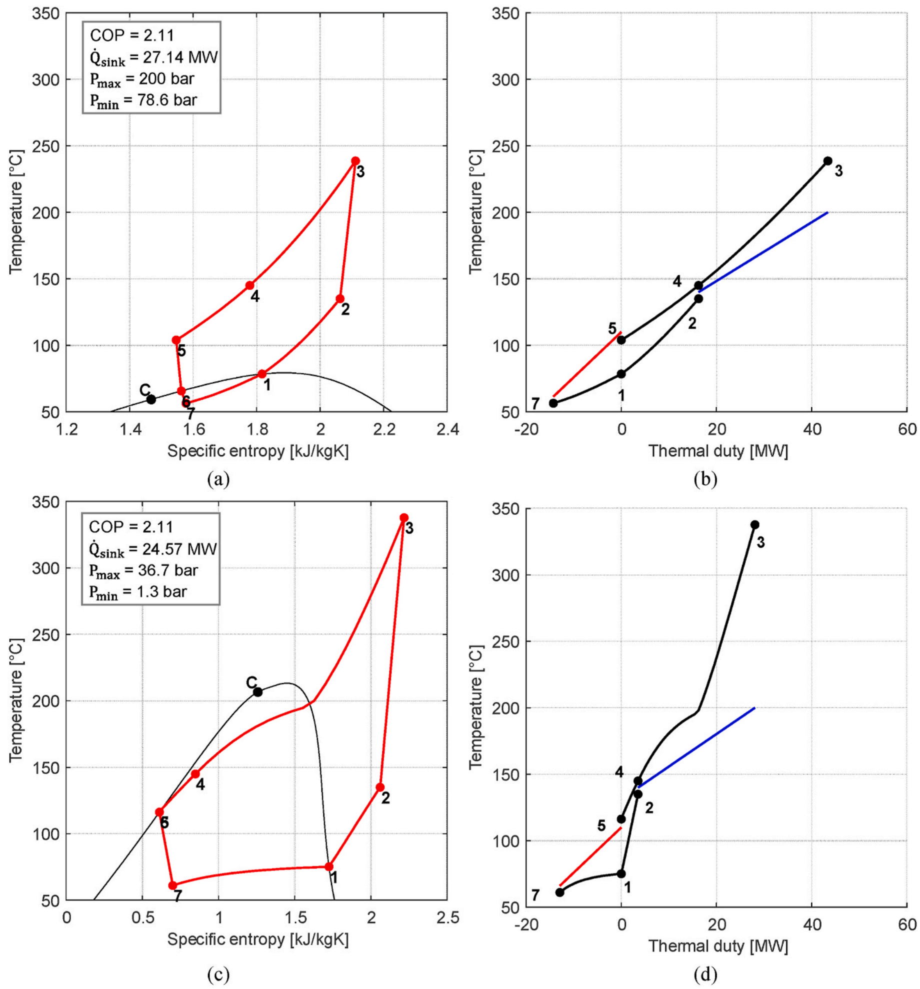

Fig. 8. HTHP from the Pareto front analysis of Fig. 6 with COP values of 2.11. Fig a, c) T-s diagrams of the cycles, b, d) T-Q diagrams of the HXs (evaporator, recuperator and cooler). CO_2-dominant mixtures in Fig a, b) with transcritical conditions, acetone-dominant mixtures in c, d) with subcritical ones.

fluid composition, a higher maximum temperature is foreseen in subcritical solutions. As a matter of fact, in all simulations from the Pareto front the subcritical HTHPs achieve a maximum temperature above the thermal stability of the working fluid (above 250 °C), even if the maximum pressures required result always below 50 bar, for any condition, whereas for the transcritical configuration it is still fixed at 200 bar.

The cycle minimum pressure ranges from 70 to 100 bar for the transcritical solutions, while remains between 0.8 and 2 bar for the subcritical ones, introducing problems related to sub-atmospheric pressures in the cycle components. The impact of the different compressor inlet pressure is evident when considering the compressor VR, being one order of magnitude higher than the value for transcritical HTHP with CO_2-dominant mixtures. Analogous considerations can be drawn for the VHC of the HTHP, that particularly favors transcritical configurations with relevant consequences on the footprint and compactness of the system. The trend of the compressor isentropic efficiency is reported in Fig. 6.g: the difference in isentropic efficiency between the transcritical and subcritical configurations is around 1.5 percentage points across the whole COP domain, with higher efficiency for lower pressure ratios (i.e. for higher COP), reflecting the detrimental effects of higher pressure ratios to the compressor efficiency.

It must be noted that this limited reduction in efficiency at relatively high pressure ratios is a consequence of the thermodynamic properties of acetone-dominant mixtures. The low heat capacity ratio of acetone vapor (γ around 1.10 to 1.12) limits the divergence of isobars on the T-s diagram, reducing the cumulative deviation between the real and isentropic compression paths even at high pressure ratios. More detailed analyses in future works could deepen these preliminary considerations, for instance, proposing compressors design and performances tuned on the working fluid characteristics.

To facilitate the interpretation of these results, a graphical comparison of representative cycle simulations is provided in the form of T-s and T-Q diagrams, explicitly illustrating the heat transfer processes within the evaporator, recuperator and cooler. Specifically, two representative regions are shown: (i) solutions with relatively high COP values (around 2.75), delivering around 10-13 MW_{th} to the sink, (ii) solutions with lower COP values (around 2.1) and a significantly higher exploitation of the heat source, leading to useful thermal powers in the range between 25 and 28 MW_{th}. The first set of operating conditions, with COP values of around 2.75, is depicted in Fig. 7, while the second one, with COP values of around 2.1, is shown in Fig. 8. In the T-Q diagrams, the heat sink is represented in blue, with a fixed temperature profile between 140 °C and 200 °C, whereas the heat source, shown in red, always enters the evaporator at 110 °C and exits the component with a variable outlet temperature, depending on the selected operating point.

Being fixed the heat source mass flow rate, its slope on the T-Q diagram (red line) is the same for all four configurations represented, while, on the other hand, the heat sink temperatures are fixed by the application, but its slope on the T-Q diagram (blue line) depends on the thermal power delivered to the heat sink, which determines the resulting

Table 6
Comparison between transcritical and subcritical HTHP configurations with the CO_2+Acetone mixture for the case study depicted in Table 4.

Parameter	Higher COP (Fig. 7)		Lower COP (Fig. 8)	
	Transcritical	Subcritical	Transcritical	Subcritical
Coefficient of Performance (COP)	2.75	2.75	2.11	2.11
Thermal Power to Sink ($\dot{Q}_{sink}$) [MW_{th}]	10.20	12.52	27.14	24.57
Maximum / Minimum Pressure [bar]	200 / 101.3	24.9 / 1.8	200 / 78.6	36.7 / 1.3
Compressor Pressure Ratio [−]	1.99	13.93	2.55	28.31
Compr. Volume Ratio (VR) [−]	1.56	11.60	1.90	21.15
Compr. Equivalent Isentropic Efficiency [%]	73.42	71.75	72.65	70.83
Volumetric Heating Capacity (VHC) [kJ/m^3]	21359	1936	19452	1446
$\Delta T_{ml,evaporator}$ [°C]	7.51	12.13	19.26	17.33
$\Delta T_{ml,cooler}$ [°C]	6.21	25.91	19.48	49.36
$\Delta T_{ml,recuperator}$ [°C]	11.58	17.97	18.87	26.16
CO_2 molar fraction [%]	84.77	6.44	93.20	17.92
Working fluid mass flow rate [kg/s]	91.87	20.13	176.56	36.77
Evaporator Outlet Temperature (T_1) [°C]	100.7	86.5	78.5	75.2
Compressor Outlet Temperature (T_3) [°C]	205.2	283.0	238.6	337.7
Heat Source Outlet Temperature [°C]	87.9	82.9	61.4	66.0
Heat Source Exploitation (ΔT_{source}) [°C]	22.1	27.1	48.6	44

mass flow rate.

It is evident that transcritical configurations require heat exchangers with larger heat transfer surfaces, due to the lower average temperature difference between the working fluid and the heat sink in the supercritical gas cooler. This effect is directly linked to the smoother temperature profile of the supercritical flow of the CO_2-rich mixture in the cooler at 200 bar (at reduced pressures higher than 2), which improves the matching with heat sink temperature profiles at the expense of increased heat transfer area. Differently, subcritical layouts exhibit maximum temperatures of the working fluid approximately 100 °C higher than those of the transcritical counterparts, resulting in concerns regarding the long-term thermal stability of the working fluid, thus improving the industrial interest in transcritical HTHP configurations.

In addition to the graphical results of the four HTHP representative of the whole solution domain of the pareto optimization, the main KPIs of the HTHPs considered in this case study are summarized in Table 6: also the logarithmic mean temperature differences across all the HX of the HTHPs are shown in the table (ΔT_{lm}) to quantitatively point to the irreversibility related to the heat transfer process in the HX of Figs. 7 and 8.

From the Table it is notable that transcritical configurations demonstrate significantly higher compactness, operating at a fixed maximum pressure of 200 bar and minimum pressures between approximately 70 and 100 bar, resulting in low pressure ratios and compressor volumetric ratios. These features are particularly attractive from a turbomachinery design perspective, as they ease compressor mechanical design and manufacturing, marking an important difference between the two configurations.

In conclusion, transcritical HTHP configurations emerge as viable solutions for applications involving highly sensible heat sinks when CO_2-based mixtures with less volatile dopants are employed. The results of the case study for production of pressurized water from 140 °C to 200 °C evidence that CO_2-rich transcritical configurations are particularly advantageous when maximizing heat source recovery and system compactness is required: if compared to subcritical configurations, they could ensure a more feasible HTHP design and operation, characterized by limited compressor pressure and volumetric ratios, limiting the maximum temperature of the working fluid thus issues related to the working fluid stability.

5. Conclusions

This work investigated the potential of CO_2-based working fluid mixtures for high-temperature heat pump applications, with a specific focus on transcritical configurations. The analysis combined a systematic parametric investigation of the HTHP at fixed mixture composition ($90\%_{molar}$ CO_2 + $10\%_{molar}$ acetone) with a detailed industrial case study, aiming to clarify the thermodynamic reasons governing performance trends and to also provide useful insights for these systems design in practical applications.

The first set of results highlighted that the transcritical HTHP performance is strongly influenced by the minimum cycle pressure and by the cooler outlet temperature, at fixed mixture composition and maximum pressure: increasing the evaporator outlet pressure shifts the heat introduction process towards higher average temperatures, reducing both the temperature lift and the compressor pressure ratio, and thus leading to higher COP values. However, this comes at the expense of a reduced exploitation of sensible heat sources, as the effective temperature glide during evaporation decreases when operating with pressures above the cricondentherm. This trade-off clearly demonstrates that transcritical CO_2-based mixtures must be tailored to the specific objective of the application, whether maximizing COP or maximizing waste heat recovery.

The analysis further showed that variations in cooler outlet temperature primarily affect the heat rejection process, increasing the temperature lift and reducing COP as the average heat rejection temperature increases. In this case, compressor volumetric ratios remain largely unaffected due to fixed pressure boundaries, whereas the volumetric heating capacity is penalized by the reduction in compressor inlet density at higher temperatures.

Building on these insights, the second part of the study applied the proposed methodology to a realistic industrial case study involving the production of pressurized hot water from 140 °C to 200 °C. By fixing the heat source and sink conditions and allowing the working fluid composition to vary, the analysis demonstrated the flexibility of CO_2-based mixtures in properly adapting to real operating constraints. The Pareto analysis clearly revealed the trade-off between COP and useful thermal power delivered to the sink, highlighting that CO_2-rich transcritical configurations are particularly effective when high waste heat exploitation and compact system design are required. Subcritical configurations, while achieving comparable COP values in some cases, exhibited significantly higher compressor pressure and volumetric ratios, very high compressor outlet temperatures, raising concerns related to component sizing and thermal stability of the working fluid.

Overall, the results confirm that the category of CO_2-based mixtures proposed represent a promising pathway for extending the operating range of HTHPs toward higher temperatures, especially in applications characterized by highly sensible heat sinks. The mixture key advantage is not only related to the respective thermodynamic performance, but also in the ability to tune the working fluid properties, such as the cricondentherm conditions, evaporation temperature glide and density through composition and pressure levels optimization. This process enables a level of design flexibility that is not achievable with pure fluids.

The present study provides a clear thermodynamic framework and practical design guidelines supporting the deployment of CO_2-based mixture HTHPs as a viable solution for industrial heat decarbonization.

From the technical point of view, uncertainties can be related to the introduction of the expander for the liquid phase before the evaporator, as the component is not standardized considering the current level of state-of-the-art technical solutions for HTHP.

Future works should extend the present analysis to additional CO_2-based mixtures with alternative dopants, in order to identify optimal working fluids for different temperature levels and application constraints. Furthermore, a dedicated experimental validation of thermodynamic and transport properties of CO_2-based mixtures is required to reduce uncertainties and to strengthen the reliability of these systems performance assessments. Similarly, future work could focus on the preliminary design of the compressors operating under the conditions investigated in this study, in order to provide more accurate efficiency estimates and to refine the comparison between transcritical and subcritical configurations. Finally, long-term thermal stability at elevated temperatures, together with detailed component design and techno-economic analyses, should be addressed to fully evaluate the feasibility and integration potential of these systems in real industrial environments.

CRediT authorship contribution statement

Dario Alfani: Writing – review & editing, Writing – original draft, Visualization, Software, Methodology, Investigation, Formal analysis, Data curation, Conceptualization. **Ettore Morosini:** Writing – review & editing, Writing – original draft, Visualization, Software, Methodology, Investigation, Formal analysis, Data curation, Conceptualization. **Giampaolo Manzolini:** Writing – review & editing, Supervision, Project administration, Funding acquisition, Conceptualization.

Declaration of competing interest

The authors declare that they have no known competing financial interests or personal relationships that could have appeared to influence the work reported in this paper.

Acknowledgments

This study was carried out within the NEST - Network 4 Energy Sustainable Transition (D.D. 1243 02/08/2022, PE00000021) and received funding under the National Recovery and Resilience Plan (NRRP), Mission 4 Component 2 Investment 1.3, funded from the European Union - NextGenerationEU. This manuscript reflects only the authors' views and opinions, neither the European Union nor the European Commission can be considered responsible for them.

This paper is part of the project HICLOPS "High-medium temperature closed power cycles for waste heat recovery and renewable sources" that has received funding from the MUR Progetti di Rilevante Interesse Nazionale (PRIN) Bando 2022 under grant No 2022HMZ39A.

The authors would like to acknowledge Mario Renzoni for the time spent during his M.Sc. thesis on the topic of high temperature heat pumps with mixtures.

APPENDIX. Validation of numerical model for HTHP with literature

The appendix highlights the validation of HTHP model developed in this work (discussed in Section 2.2) with the results of the model adopted and presented by Abedini in literature [22], under the boundary conditions on heat source and heat sink listed in Table 4 and the same assumptions on the cycle characteristics (isentropic efficiencies, pressure levels, plant layout, etc) of the one used in Abedini's work. The validation is done by directly reproducing selected subcritical HTHP conditions from Abedini for three working fluid mixtures with non negligible glides during evaporation.

The results, summarized in the table, show an excellent agreement for all reported KPIs, hence validating the numerical routine adopted in this study.

Table A1
Validation of the model for HTHP of this work with literature results

Subcritical HTHP Parameter	This work	Abedini [22]
Working Fluid	Toluene/Ethanol (x_{Tolu} = 67%)	
COP	3.89	3.89
VHC [kJ/m^3]	1414	1416
Compressor outlet temperature [°C]	224	224
Evaporation temperature glide [°C]	17.7	17.8
Condensation temperature glide [°C]	30.1	30.2
Working Fluid	Benzene/M-xylene (x_{Benz} = 56%)	
COP	3.75	3.75
VHC [kJ/m^3]	816	815
Compressor outlet temperature [°C]	216	216
Evaporation temperature glide [°C]	18.4	18.4
Condensation temperature glide [°C]	17.6	17.6
Working Fluid	Methanol/Ethyl benzene (x_{Meth} = 80%)	
COP	3.66	3.67
VHC [kJ/m^3]	2456	2463
Compressor outlet temperature [°C]	276	276
Evaporation temperature glide [°C]	19.6	19.5
Condensation temperature glide [°C]	20.0	19.9

Data availability

Data will be made available on request.

References

[1] Wieland C, Schifflechner C, Dawo F, Astolfi M. The organic Rankine cycle power systems market: recent developments and future perspectives. Appl Therm Eng Apr. 2023;224:119980. https://doi.org/10.1016/J.APPLTHERMALENG.2023.119980.

[2] Forman C, Muritala IK, Pardemann R, Meyer B. Estimating the global waste heat potential. Renew Sustain Energy Rev May 2016;57:1568–79. https://doi.org/10.1016/J.RSER.2015.12.192.

[3] KCORC. Thermal energy harvesting - the path to tapping into a large CO2-free European power source [Online]. Available: www.kcorc.org/en/committees/thermal-energy-harvesting-advocacy-group/; 2022.

[4] Arpagaus C, Bless F, Uhlmann M, Schiffmann J, Bertsch SS. High temperature heat pumps: market overview, state of the art, research status, refrigerants, and application potentials. Energy Jun. 2018;152:985–1010. https://doi.org/10.1016/J.ENERGY.2018.03.166.

[5] de Boer Robert. Strengthening industrial heat pump innovation decarbonizing industrial heat [Online]. Available: https://www.sintef.no/globalassets/sintef-energi/industrial-heat-pump-whitepaper/2020-07-10-whitepaper-ihp-a4.pdf. [Accessed 14 July 2025].

[6] Marina A, Spoelstra S, Zondag HA, Wemmers AK. An estimation of the European industrial heat pump market potential. Renew Sustain Energy Rev Apr. 2021;139:110545. https://doi.org/10.1016/J.RSER.2020.110545.

[7] Wu D, Jiang J, Hu B, Wang RZ. Experimental investigation on the performance of a very high temperature heat pump with water refrigerant. Energy Jan. 2020;190:116427. https://doi.org/10.1016/j.energy.2019.116427.

[8] Wu D, Wei J, Hu B. Theoretical analysis, experimental research and industrial verification of high temperature heat pump based on R1233zd(E). Energy Mar. 2025;319:135175. https://doi.org/10.1016/j.energy.2025.135175.

[9] Mateu-Royo C, Navarro-Esbrí J, Mota-Babiloni A, Amat-Albuixech M, Molés F. Theoretical evaluation of different high-temperature heat pump configurations for low-grade waste heat recovery. Int J Refrig Jun. 2018;90:229–37. https://doi.org/10.1016/j.ijrefrig.2018.04.017.

[10] Obika E, Heberle F, Brüggemann D. Thermodynamic analysis of novel mixtures including siloxanes and cyclic hydrocarbons for high-temperature heat pumps. Energy May 2024;294:130858. https://doi.org/10.1016/j.energy.2024.130858.

[11] Bamigbetan O, Eikevik TM, Nekså P, Bantle M, Schlemminger C. The development of a hydrocarbon high temperature heat pump for waste heat recovery. Energy Apr. 2019;173:1141–53. https://doi.org/10.1016/j.energy.2019.02.159.

[12] Hua J, et al. Study on the hydrocarbon mixtures in high-temperature heat pump systems for industrial waste heat recovery. Energy Oct. 2025;334:137886. https://doi.org/10.1016/j.energy.2025.137886.

[13] Shi L, et al. A comprehensive analysis of novel environmentally friendly refrigerants in high-temperature heat pumps for industrial heating. Energy Dec. 2025;341:139493. https://doi.org/10.1016/j.energy.2025.139493.

[14] Brendel LPM, Bernal SN, Arpagaus C, Roskosch D, Bardow A, Bertsch SS. Experimental performance comparison of high-glide hydrocarbon and synthetic refrigerant mixtures in a high-temperature heat pump. Energies Apr. 2024;17(8):1981. https://doi.org/10.3390/EN17081981.

[15] Spale J, Hoess AJ, Bell IH, Ziviani D. Exploratory study on Low-GWP working fluid mixtures for industrial high temperature heat pump with 200 °C supply temperature. Energy Aug. 2024:132677. https://doi.org/10.1016/J.ENERGY.2024.132677.

[16] Brendel LPM, et al. High-glide refrigerant blends in high-temperature heat pumps: part 1 – coefficient of performance. Int J Refrig Sep. 2024;165:84–96. https://doi.org/10.1016/J.IJREFRIG.2024.05.005.

[17] Zhang T, Wang Y, Liu J, Cheng J, Zhang X. Study on CO2 zeotropic mixture heat pump for waste heat deep recovery - energy and exergy analysis. Energy Aug. 2025;329:136662. https://doi.org/10.1016/j.energy.2025.136662.

[18] Ganesan P, Eikevik TM. New zeotropic CO2-based refrigerant mixtures for cascade high-temperature heat pump to reach heat sink temperature up to 180 °C. Energy Convers Manag X Oct. 2023;20:100407. https://doi.org/10.1016/J.ECMX.2023.100407.

[19] Gómez-Hernández J, Grimes R, Briongos JV, Marugán-Cruz C, Santana D. Carbon dioxide and acetone mixtures as refrigerants for industry heat pumps to supply temperature in the range 150–220 oC. Energy Apr. 2023;269:126821. https://doi.org/10.1016/J.ENERGY.2023.126821.

[20] Zhou F, Zhang T, Wei D, Liu J, Zhang X. Optimal refrigerant selection and parameter analysis of a wastewater heat pump using CO2 zeotropic mixtures. Appl Therm Eng Sep. 2024;253:123789. https://doi.org/10.1016/J.APPLTHERMALENG.2024.123789.

[21] IEA Technology Collaboration Programme. Annex 58 high-temperature heat pumps final report [Online]. Available: https://heatpumpingtechnologies.org/publications/annex-58-high-temperature-heat-pumps-final-report/. [Accessed 23 December 2025].

[22] Abedini H, et al. A comprehensive analysis of binary mixtures as working fluid in high temperature heat pumps. Energy Convers Manag Feb. 2023;277:116652. https://doi.org/10.1016/J.ENCONMAN.2022.116652.

[23] Vieren E, Demeester T, Beyne W, Arteconi A, De Paepe M, Lecompte S. The thermodynamic potential of high-temperature transcritical heat pump cycles for industrial processes with large temperature glides. Appl Therm Eng Nov. 2023;234:121197. https://doi.org/10.1016/J.APPLTHERMALENG.2023.121197.

[24] Bang-Møller C, Rokni M, Elmegaard B, Ahrenfeldt J, Henriksen UB. Decentralized combined heat and power production by two-stage biomass gasification and solid oxide fuel cells. Energy Sep. 2013;58:527–37. https://doi.org/10.1016/J.ENERGY.2013.06.046.

[25] Zühlsdorf B, Bühler F, Bantle M, Elmegaard B. Analysis of technologies and potentials for heat pump-based process heat supply above 150 °C. Energy Convers Manag X Apr. 2019;2:100011. https://doi.org/10.1016/J.ECMX.2019.100011.

[26] Wang JF, Brown C, Cleland DJ. Heat pump heat recovery options for food industry dryers. Int J Refrig 2018;86:48–55. https://doi.org/10.1016/j.ijrefrig.2017.11.028.

[27] Arpagaus Cordin, Bless Frédéric, Bertsch Stefan. Integration of high-temperature heat pumps in Swiss industrial processes (HTHP-CH). In: 14th IEA heat pump conference , Chicago; 2023.

[28] Barco-Burgos J, Bruno JC, Eicker U, Saldaña-Robles AL, Alcántar-Camarena V. Review on the integration of high-temperature heat pumps in district heating and cooling networks. Energy Jan. 2022;239:122378. https://doi.org/10.1016/J.ENERGY.2021.122378.

[29] Passamonti A, Sachse F, Bombarda P, Bracke R. Design, construction, and commissioning of a 500 kW high-temperature heat pump plant for the district heating network of Bochum, Germany. Energy Rep Jun. 2025;13:548–61. https://doi.org/10.1016/J.EGYR.2024.11.080.

[30] Wolscht L, Knobloch K, Jacquemoud E, Jenny P. Dynamic simulation and experimental validation of a 35 MW heat pump based on a transcritical CO2 cycle. Energy May 2024;294:130897. https://doi.org/10.1016/J.ENERGY.2024.130897.

[31] Wolscht L, Podeur M, Adam M, Jacquemoud E. Off-design heat exchanger modelling for Transcritical CO_2 heat pump cycles. In: ASME turboexpo; 2024.

[32] Held Timothy J, Miller Jason, Mallinak Jason, Magyar Luke. High-Temperature Industrial-Scale CO2 Heat Pumps: Thermodynamic Analysis and Pilot-Scale Testing. J. Eng. Gas Turbines Power Oct 2025;147(10):101010. https://doi.org/10.1115/1.4068029. Published Online: March 21, 2025.

[33] Morosini E, et al. Analysis of the CO2 + C2Cl4 mixture in high temperature heat pumps: experimental thermal stability, liquid densities and cycle simulations. Energy Convers Manag Dec. 2024;322:119145. https://doi.org/10.1016/J.ENCONMAN.2024.119145.

[34] Morosini E, Alfani D, Renzoni M, Manzolini G. Thermally integrated innovative carnot batteries to upgrade and dispatch low temperature sensible waste heat. In: Journal of physics: conference series. IOP Publishing; Nov. 2024, 012056. https://doi.org/10.1088/1742-6596/2893/1/012056.

[35] Sanz Garcia L, Jacquemoud E, Jenny P. Thermo-economic heat exchanger optimization for electro-thermal energy storage based on transcritical CO2 cycles. In: 3rd european conference on supercritical CO2 (sCO2) power systems 2019: 19th-20th September 2019; Oct. 2019. p. 353–62. https://doi.org/10.17185/DUEPUBLICO/48917.

[36] MAN heat pump [Online]. Available: https://www.man-es.com/docs/default-source/document-sync/man-heat-pump-hpu328c592b5d584f9eba47f4b6bed3574e.pdf?sfvrsn=9bd416fb_3. [Accessed 20 February 2024].

[37] Held TJ, Miller JD, Mallinak JA, Magyar L. High temperature CO2 heat pumps for industrial process heat applications. In: The 8th international supercritical CO2 power cycles symposium; 2024. Paper #61.

[38] Dostal V, Driscoll MJ, Hejzlar P. A supercritical carbon dioxide cycle for next generation nuclear reactors. Techn Rep MIT-ANP-TR-100 2004:1–317. doi: MIT-ANP-TR-100.

[39] La Porte Demonstration Facility - net Power.".

[40] Shamsi SSM, Barberis S, Maccarini S, Traverso A. Large scale energy storage systems based on carbon dioxide thermal cycles: a critical review. Renew Sustain Energy Rev Mar. 2024;192:114245. https://doi.org/10.1016/J.RSER.2023.114245.

[41] Held TJ, et al. Compressor development for CO2-Based pumped thermal energy storage systems. J Eng Gas Turbines Power Sep. 2025;147(9). https://doi.org/10.1115/1.4067449.

[42] Kunz O, Wagner W. The GERG-2008 wide-range equation of state for natural gases and other mixtures: an expansion of GERG-2004. J Chem Eng Data Nov. 2012;57(11):3032–91. https://doi.org/10.1021/je300655b.

[43] Cullimore I, Lemmon EW. Generalized mixing model (KW0) parameters for acetone and carbon dioxide in Refprop 10. 2010.